iScience, Volume *23*

Supplemental Information

Tunneling Nanotubes Mediate Adaptation of Glioblastoma Cells to Temozolomide and Ionizing Radiation Treatment

Silvana Valdebenito, Alessandra Audia, Krishna P.L. Bhat, George Okafo, and Eliseo A. Eugenin

Supplemental Information

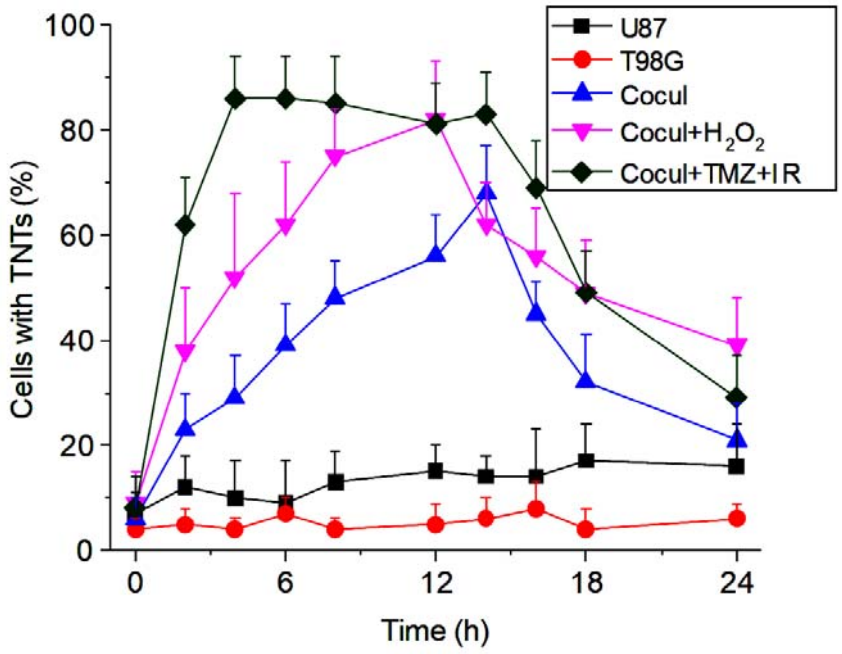

Figure S1 (Related to Figure 1). TNTs are induced in our co-culture system upon oxidative stress or TMZ/IR treatment. Quantification of TNTs in our co-culture system in response to H_2O_2, IR, and TMZ. All data were expressed as mean±S.D.

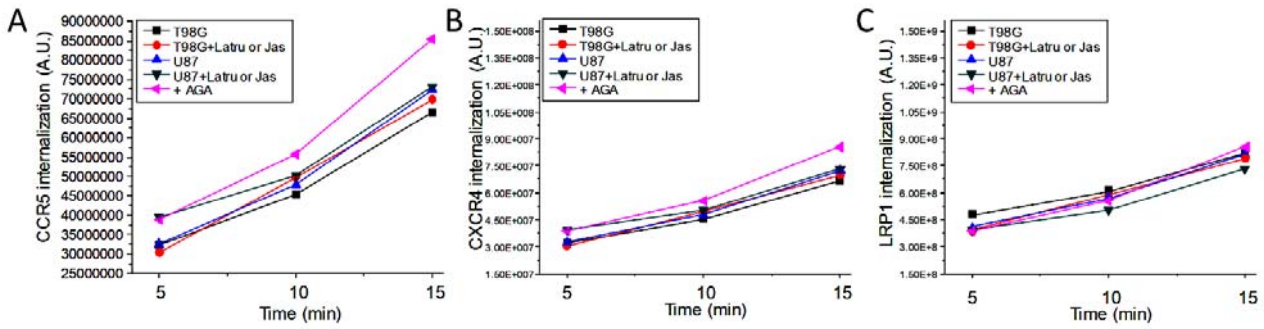

Figure S2 (Related to Figure 1 and 2). Internalization experiments using biotinylated antibodies for CCR5 (A), CXCR4 (B), and LRP1 (C) in the function of time in the presence and absence of mild actin or gap junction blockers that reduce the formation of TNTs and/or associated transport. No differences in receptor internalization were observed with any of the treatments used to block TNTs. The main reason to observe a strong effect of these blockers on TNT formation and transport is the high amount of actin polymerization required for TNT formation, associated transport, and collapse of the process. This highly dependent mechanism on actin only has been described at this magnitude in cell division and TNT formation. Thus, our blockers at the concentration used do not affect the trafficking of high recycling receptor types on the plasma membrane that relay on active actin signaling and a significant rate of polymerization and de-polymerization. n=4, data were expressed as mean±S.D.

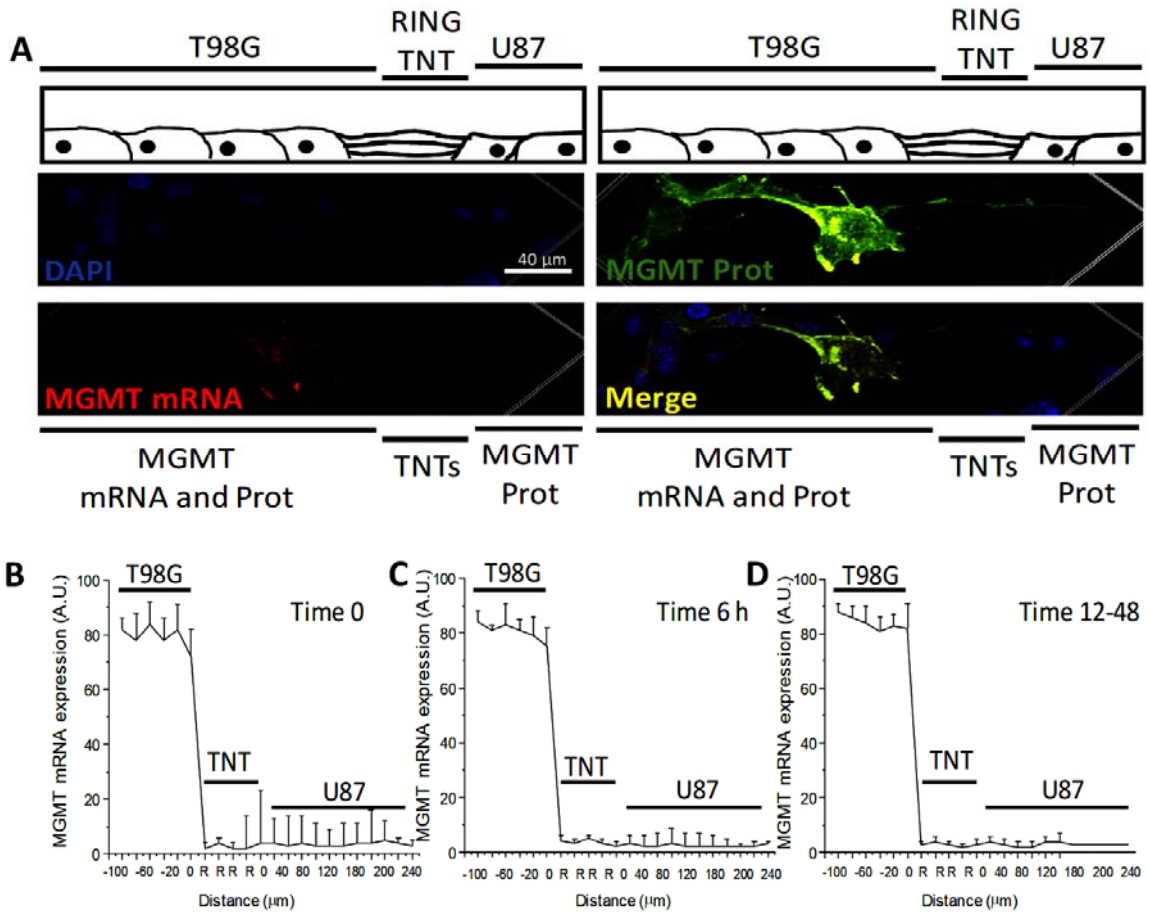

Figure S3 (Related to Figure 4). MGMT mRNA is not transported via TNTs. The time course of MGMT mRNA spread between resistant and sensitive cells to treatment. Immune staining for GAP43 or protein 14-3-3γ, both TNT markers, DAPI, MGMT protein, and MGMT mRNA analysis by confocal microscopy of our co-culture system. (A) The cartoon represents our co-culture system and corresponding confocal images for DAPI, MGMT protein, mRNA, and the merge of all colors at the interface after TMZ and IR treatment. (B) Quantification of positive pixels for MGMT mRNA in our confocal images using our co-culture system at time 0 before TMZ and IR treatment. (C) Quantification of MGMT mRNA up to 6 h post-TNT formation. (D) Corresponds to the diffusion of MGMT mRNA into TNTs and U87 cells after 12 to 48 h post-TMZ/IR treatment. n=4-5.

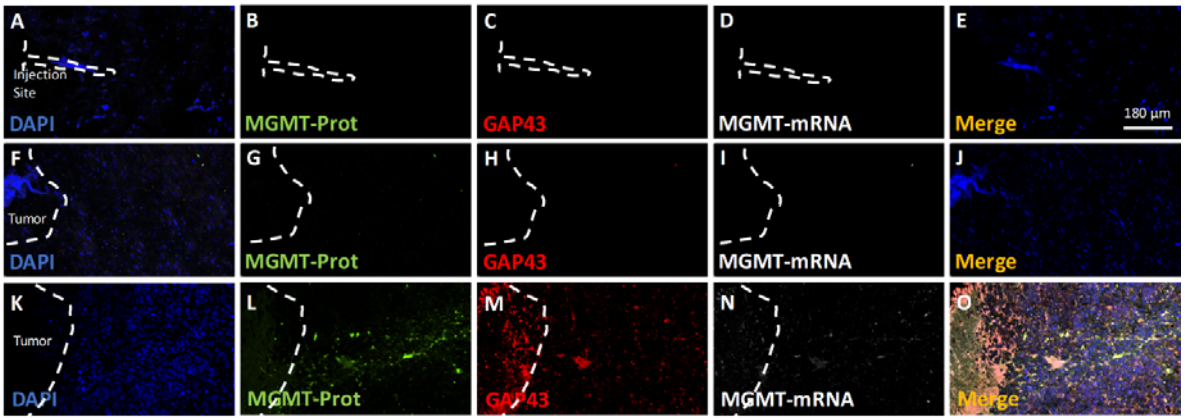

Figure S4 (Related to Figure 5): Glioblastoma stem-like cells were isolated from patients undergoing surgery at M.D. Anderson Medical Center and injected into the cortex of mice to generate an orthotopic xenograft animal. Tissue sections were stained for nuclei (DAPI, blue staining), MGMT protein (MGMT-Prot, green staining), GAP43 (red), and MGMT mRNA (white staining) as well as the merge of all colors. (A-E) Mice cortex with no injected cells to demonstrate the specificity of the staining and tumor growth. (F-G) Injection of glioblastoma cells (negative for MGMT) into the cortex with non-unspecific staining. (K-O) Microinjection of glioblastoma stem-like cells into the cortex and diffusion of MGMT protein into the mice cortex from the primary tumor in association with GAP43 expression. Segmented lines denote the border of the tumor or injection site (n=3-5).

Tables

Table S1 (Related to Figure 1 and 2): TNT Characteristic in Cell Lines

Condition	TNT stability (min)	TNT Length (µm)	TNT vesicular transport (% of TNTs)	TNT Branching (% of TNTs)
U87-Control	1.65±0.98 (T) 2.31±0.25 (S)	8.55±3.69 (Sh) 38.25±11.6 (Lo)	0.12±0.05	0±0
U87-H_2O_2	3.65±2.67 (T) 18.65±10.1 (S)	19.3±11.0 (Sh) 99.4±21.2 (Lo)	5.04±2.39	1.02±0.23
U87-IR	28.05±21.23(T) 161.01±87.1(S)	17.04±11 (Sh) 256.99±101 (Lo)	10.02±3.66	11.45±3.33
U87-TMZ	5.66±2.36(T) 31.09±11.1(S)	20.05±8.8 (Sh) 45.85±10.1 (Lo)	0.58±0.08	1.57±0.89
U87-IR+TMZ	26.81±10.8(T) 125.6±29.9(S)	23.3±9.08 (Sh) 111±20.6 (Lo)	15.78±7.88±	16.87±8.47
T98G-Control	1.09±1.05(T) 2.08±0.85(S)	6.78±2.89 (Sh) 22.28±6.79 (Lo)	0.17±0.11	0±0
T98G-H_2O_2	2.87±0.98(T) 15.58±5.08 (S)	23.09±10.1 (Sh) 112.85±20.9(Lo)	8.09±3.69	3.68±1.08
T98G-IR	35.85±10.58(T) 159.87±20.1(S)	28.8±7.09 (Sh) 269.78±36.9(Lo)	16.98±9.78	21.05±8.09
T98G-TMZ	6.71±2.01(T) 29.89±8.87(S)	26.78±10.5 (Sh) 39.87±8.88 (Lo)	1.68±0.98	2.68±1.05
T98G- IR+TMZ	35.91±8.67(T) 89.78±10.7(S)	28.98±4.58 (Sh) 165.5±29.8 (Lo)	19.87±6.78	19.7±5.68
Co-Control	2.09±1.08(T) 4.52±2.78(S)	12.69±4.51 (Sh) 35.65±8.24 (Lo)	3.05±11.85	0±0
Co-H_2O_2	6.72±2.78(T) 25.98±7.05 (S)	41.1±8.98 (Sh) 168.5±30.2 (Lo)	9.78±4.05	2.22±1.05
Co-IR	49.98±7.09(T) 198.7±29.8(S)	45.71±12.3 (Sh) 284.6±29.7 (Lo)	29.58±9.87	30.89±10.08
Co-TMZ	39.78±9.78(T) 177.8±40.9(S)	39.9±4.01 (Sh) 120.0±36.5 (Lo)	3.5±1.98	2.08±0.68
Co-IR+TMZ	46.98±10.8(T) 200.98±19.8(S)	59.8±6.54 (Sh) 298.85±84.2(Lo)	39.87±5.05	30.36±9.99

Notes: (T) Transient, (S) stable, (Sh) Short, (Lo) Long

Data were expressed as mean±S.D., n=12-15. Data were pooled during the time course examined (0 to 48 h post-treatment).

Table S2 (Related to Figure 2): Characteristic of the cell types used

Cell type	TMZ sensitive	Radiation Sensitive	MGMT expression
U87 cells	10 μM	Yes	Low
T98G	≥500 μM	No	High

Table S3: Patient information (brain and breast cancer, related to Figure 5)

Patient-condition	Age	Sex	IDH status	Cancer-grade
Healthy				
Healthy 1	42	M	Unknown	N/A
Healthy 2	49	M	Unknown	N/A
Healthy 3	59	M	Unknown	N/A
Healthy 4	55	F	Unknown	N/A
Brain Tumors				
Oligodendroglioma	42	M	Unknown	2
Astrocytoma	46	M	R132H	2
Astrocytoma	35	F	Unknown	3
Astrocytoma	61	M	Unknown	3
Glioblastoma	55	F	Unknown	4
Oligoastrocytoma	36	M	Unknown	2
Breast Cancer				
Invasive Ductal Carcinoma	51	F	Unknown	2
Invasive Ductal Carcinoma	42	F	Unknown	3
Invasive Ductal Carcinoma	33	F	Unknown	2
Invasive Ductal Carcinoma	38	F	Unknown	2
Invasive Ductal Carcinoma	47	F	Unknown	3

Transparent Methods

Materials: DMEM, fetal bovine serum (FBS), penicillin/streptomycin (P/S), and trypsin-EDTA were from Thermo-Fisher (Grand Island, NY). Purified mouse IgG_{2B} and IgG_1 myeloma proteins were from Cappel Pharmaceuticals, Inc. DAPI, anti-rabbit, and anti-mouse conjugated to Alexa were from Thermo-Fisher (Eugene, OR). The *in situ* cell death detection kit (TUNEL) was from Roche (Mannheim, Germany).

Glioblastoma Cell Lines: Cell lines, U87, and T98G were purchased from the ATCC (Manassas, VA). U87 and T98G were grown in DMEM medium supplemented with 2-10% FBS and pen/strep and maintained at 37°C in a humidified incubator supplied with 5% CO_2. Mycoplasma test was performed every 4 months, as well as new cell batches, which were ordered from the ATCC for scientific rigor.

Cell culture and IR. To perform these experiments, we used the Stem cell Isolation and Xenotransplantation Core Facility at the Albert Einstein College of Medicine (Bronx, NY). The equipment used was a Shepherd Mark I Irradiator Model 68 filed with 4000-6000 of Cesium (Ci) 137. Single-dose exposure ranged from 0 to 12 Gy. After IR, the medium was changed, and fresh medium was added. The cells were incubated for 2 or 7 days to detect clonal expansion and degree of apoptosis, as previously described (Chalmers et al., 2009). Using these cells, a co-culture model was set between T98G cells at the center of the plate, while U87 sensitive cells to treatment were at the periphery of the plate. The main reasons to perform this co-culture were to maximize the numbers of TNTs per area (interface), a localized formation (easier isolation), and directed communication.

Clinical Tissue sample collection. Human brain tissues were obtained from M.D. Anderson Medical Center. Normally, we obtained resected brain tissues with the core tumor and the edge as well as some small sections of “healthy” tissue. All our studies were approved by the M.D. Anderson and UTMB institutional review board. Tissues were obtained from astro- and oligodendroglioma stages III and IV (see Table 3). Tissues were immediately transferred to Biological safety Class II cabinet and dissected into different regions and fixed in 10 % neutral buffered formalin for at least 24 h, dehydrated, and paraffin-embedded. Serial sections from each block were prepared for Hematoxylin and Eosin staining, and the stained slides were imaged at 20X using an image capture device (Hamamatsu, Japan), and images were reviewed by an experienced pathologist.

qRT-PCR. Total RNA was extracted from GBM cells using TRIzol and the phase-lock system (Eppendorf, Hauppauge, NY, USA), following the manufacturer’s instructions. cDNA synthesis was performed using 2 µg total RNA using the iScript cDNA synthesis kit (Bio-Rad, Hercules, CA, USA) according to the manufacturer’s instructions. The amplified cDNA was used to amplify and quantify MGMT and GAPDH mRNA expression by qPCR using Absolute Blue qPCR SYBR low ROX mix in a StepOnePlus thermocycler (Applied Biosystems, Life Technologies, Carlsbad, CA, USA). The primers used correspond to GAPDH forward: 5′-GAGAAGTATGACAACAGCCTCAA-3′, GAPDH reverse: 5′AGTCCTTCCACGATACCAAAG-3′; MGMT forward: 5′- GTGATTTCTTACCAGCAATTAGCA -3′, MGMT reverse: 5′-CTGCTGCAGACCACTCTGTG -3′. The program used was denaturation for 15 min at 95°C and 40 cycles of denaturation, 15 s at 95°C; anneal, 30 s at 60°C; and amplification, 30 s at 72°C. Expression was determined using the ΔΔCT method, according to the CT values.

Live Cell Imaging. For analysis two different cell culture systems were used — first, single-cell cultures in regular tissue culture plates. Confluence used was 50 to 70 % to enable TNT extension and communication and reduce the possibility of overgrowth that can compromise TNT identification and characterization. Our imaging system corresponds to an Axio-observed Z1 with 3 redundant incubation systems with CO_2 and humidity control to avoid any significant variations in temperature, CO_2, or humidity. We imaged for 24 to 48 h, recording every 30 seconds to 1 min.

Image analysis. Raw data for TNTs and other membrane protrusions were obtained using the Zen software (Zeiss Software, Germany). As described in the result section, several rules were considered to identify a TNT. The more important was cell to cell distance and cell to cell communication by live-cell imaging. Filopodium did not comply with these rules. For confocal analysis, 3D deconvolutions were obtained using NIS elements (Nikon, Japan). Quantification of colocalization, intensities, and lengths, as well as stability, was performed in NIS elements and Image J using the criteria described in the result section.

Laser capture microdissection. Pure cultures or co-cultures of cells were grown on director slices (Expression Pathology, Culver City, CA) for laser capture. To preserve TNTs structure and communication, we fix the cells in 1.5 % PFA, and then we increased the concentration to 3.0 % after 20 min, later we added 100% ethanol to dry the slides and proceed to cut the TNTs. Most isolation was performed under control

conditions or co-cultures to reach 7,000 TNTs isolated per condition for qRT-PCR and Western blot for the MGMT protein. To perform the isolations, we used LMD6000 equipment with the respective software (Leica, Germany). For Western blot and mRNA, the polled samples were dissolved in RIPA lysis buffer, and then RNA was isolated using the RNeasy Micro Kit (Qiagen, #74004, Valencia, CA). RNA content was determined using a Nanodrop 2000 spectrophotometer (Thermo Scientific, Wilmington, DE).

Western Blot Analysis. Cells or laser captured material were lysed with RIPA buffer (Cell Signaling, Beverly, MA) containing protease and phosphate inhibitors (Cell Signaling, Danvers, MA), and 100 µg (or total collected material in the case of laser capture microdissection) of protein were electrophoresed on a 4-20% polyacrylamide gel (Bio-Rad, CA), and transferred to nitrocellulose membranes. Membranes were probed with rabbit monoclonal antibodies to MGMT (Thermofisher, Carlsbad, CA), actin (Santa Cruz Biotechnology, Dallas, TX), and GAPDH (Cell Signaling, Danvers, MA). Densitometric analysis was performed using NIH ImageJ software.

Immunofluorescence. Human GBM cells were grown on glass coverslips, fixed and permeabilized in 70% ethanol for 20 min at -20^{o}C. Cells were incubated in blocking solution for 30 min at room temperature and then in primary antibody (anti-GAP43, anti-14-3-3γ, and anti-MGMT, or isotype controls: both 1:50) overnight at 4^{o}C. Cells were washed several times with PBS at room temperature and incubated with phalloidin conjugated to Texas Red to identify actin filaments and/or the appropriate secondary antibody conjugated to FITC (Sigma, St. Louis, MO) for 1 h at room temperature,

followed by another wash in PBS for 1 h. Cells were then mounted using antifade reagent with DAPI, and cells were examined by confocal microscopy using an A1 Nikon confocal microscope with spectral detection (Tokyo, Japan). To ensure proper staining, several negative and positive controls were used as well as matching antibody isotypes, as we described (Prevedel et al., 2019). Some of the controls included MGMT negative and positive tumors, pre-absorption with the recombinant protein, and isolation for laser capture and proteomics. In all our experiments, no unspecific staining was observed.

Electron microscopy. Cells were fixed for 30 min at RT using 4% paraformaldehyde, 2% glutaraldehyde, buffered with 0.1 M sodium cacodylate. Cells were dried with hexamethyldisilazane until fully dry under a fume hood. The cells were analyzed using a Zeiss SUPRA 40 field emission scanning electron microscopy (SEM) and placed on a fitted mold for the holder. The holder was calibrated, and cells were imaged at various magnifications, as indicated, with an accelerating voltage of 3 kV. This protocol allows us to maintain TNT structure and cell shape (see details in the result section).

RNA scope for MGMT mRNA. RNAscope (RNAscope® Fluorescent Multiplexed reagent kit, Advanced Cell Diagnostics) was used as per the manufacturer's protocol and adjusted for dual detection of MGMT protein and TNT markers by immunofluorescence, as we recently described for HIV conditions (Castellano et al., 2019; Ganor et al., 2019; Prevedel et al., 2019).

Orthotopic Xenograft Animal Models. Glioblastoma stem-like cells were isolated from patients undergoing surgery at M.D. Anderson Medical Center. 500K cells were injected into the

cortex and sacrificed upon showing signs of brain disease as indicated (Moreno et al., 2017). Mice that presented neurological symptoms (i.e., seizures, inactivity, or ataxia) or that were moribund were sacrificed, and brains were fixed in formalin and stained with H&E to confirm the presence of a tumor. All animal procedures were reviewed and approved by the Institutional Animal Care and Use Committee at M.D. Anderson, Texas.

Statistical analysis. Information on the statistical tests used, and the exact values of n (number of experiments) can be found in Figure Legends. All statistical analyses were performed using GraphPad Prism 6.0 (GraphPad Software Inc.). The statistical tests were chosen according to the following: two-tailed paired or unpaired t-test was applied on datasets with a normal distribution (Kolmogorov-Smirnov test), whereas two-tailed Mann-Whitney (unpaired test) or Wilcoxon matched-paired signed-rank tests were used otherwise. $p < 0.05$ was considered as the level of statistical significance.

REFERENCES

Castellano, P., Prevedel, L., Valdebenito, S., and Eugenin, E.A. (2019). HIV infection and latency induce a unique metabolic signature in human macrophages. Sci Rep *9*, 3941.
Chalmers, A.J., Ruff, E.M., Martindale, C., Lovegrove, N., and Short, S.C. (2009). Cytotoxic effects of temozolomide and radiation are additive- and schedule-dependent. Int J Radiat Oncol Biol Phys *75*, 1511-1519.
Ganor, Y., Real, F., Sennepin, A., Dutertre, C.A., Prevedel, L., Xu, L., Tudor, D., Charmeteau, B., Couedel-Courteille, A., Marion, S.*, et al.* (2019). HIV-1 reservoirs in urethral macrophages of patients under suppressive antiretroviral therapy. Nat Microbiol *4*, 633-644.
Moreno, M., Pedrosa, L., Pare, L., Pineda, E., Bejarano, L., Martinez, J., Balasubramaniyan, V., Ezhilarasan, R., Kallarackal, N., Kim, S.H.*, et al.* (2017). GPR56/ADGRG1 Inhibits Mesenchymal Differentiation and Radioresistance in Glioblastoma. Cell reports *21*, 2183-2197.
Prevedel, L., Ruel, N., Castellano, P., Smith, C., Malik, S., Villeux, C., Bomsel, M., Morgello, S., and Eugenin, E.A. (2019). Identification, Localization, and Quantification of HIV Reservoirs Using Microscopy. Curr Protoc Cell Biol *82*, e64.

Reagents

Reagent or Resource	Source	Identifier
Antibodies		
Anti-Human GAP43 /EP890Y	Abcam	Cat# ab75810; https://www.abcam.com/gap43-antibody-ep890y-ab75810.html#top-600
Anti-Human 14-3-3 gamma/YWHAG	Abcam	Cat# ab155050; https://www.abcam.com/14-3-3-gammaywhag-antibody-ab155050.html
GAPDH (14C10) anti-Human	Cell Signaling	Cat# 2118L; https://media.cellsignal.com/pdf/2118.pdf
MGMT Anti-Human (MT23.3)	Invitrogen/Thermo Fisher Scientific	Cat# RL242361; RRID: AB_2533219
Actin (C-2) Anti-Human	Santa Cruz Biotechnology	Cat# SC-8432; https://datasheets.scbt.com/sc-8432.pdf
Anti-Human Connexin 43	Sigma Aldrich	Cat# C6219; https://www.sigmaaldrich.com/content/dam/sigma-aldrich/docs/Sigma/Datasheet/3/c6219dat.pdf
Normal Anti-Mouse Igg	Santa Cruz Biotechnology	Cat# SC-2025; https://datasheets.scbt.com/sc-2025.pdf
Normal Anti-Rabbit Igg	Sigma Aldrich	Cat# A-9919; https://www.sigmaaldrich.com/content/dam/sigma-aldrich/docs/Sigma/Datasheet/6/a9919dat.pdf
Donkey Anti-Rabbit, Alexa Fluor 488	Invitrogen/Thermo Fisher Scientific	Cat# A21206; RRID: AB_2535792
Goat Anti-Mouse, Alexa Fluor 568	Invitrogen/Thermo Fisher Scientific	Cat# A11031; RRID: AB_144696
Chemicals, Peptides, and Recombinant Proteins		
Human MGMT protein	Abcam	Cat# ab79251
Critical Commercial Assays		
RNAScope Probe-Hs-MGMT	ACDbio	Cat# 588941
DAPI	Thermo Fisher Scientific	Cat# P36931
SuperSignal WestPico Chemiluminescent	Thermo Fisher Scientific	Cat# 34080
Biological Samples		
Patients GB	MD Anderson	N/A

Tissue Samples	Medical School, Houston, Texas	
Cell Lines		
U87 MG	ATCC	Cat# HTB-14
T98G	ATCC	Cat# CLR-1690
Software		
ImageJ	ImageJ	https://imagej.nih.gov/ij/
OriginLab 2019	Origin	https://www.originlab.com/
NIS-elements 2.3	Nikon	https://www.microscope.healthcare.nikon.com/products/software
ZEN 4.7	Zeiss	https://www.zeiss.com/microscopy/us/products/microscope-software/zen.html